Supporting Information

Direct synthesis of organic salt-derived porous carbons for enhanced CO_2 and methane storage

Ibtisam Alali, and Robert Mokaya*

School of Chemistry, University of Nottingham, University Park, Nottingham NG7 2RD, U. K.

E-mail: r.mokaya@nottingham.ac.uk (R. Mokaya)

Table S1. CO_2 uptake capacity of various porous carbons at 25 °C and 0.15 bar or 1 bar (The data in the table is adapted from reference 11 in main manuscript).

	CO_2 uptake (mmol/g)		Reference
	1 bar	0.15 bar	
Sawdust-derived activated carbon	4.8	1.2	1
Petroleum pitch-derived activated carbon	4.55	~1.0	2
Activated carbon spheres	4.55	~1.1	3
Phenolic resin activated carbon spheres	4.5	~1.2	4
Fungi-derived activated carbon	3.5	~1.0	5
Chitosan-derived activated carbon	3.86	~1.1	6
Polypyrrole derived activated carbon	3.9	~1.0	7
Soya bean derived N-doped activated carbon	4.24	1.2	8
N-doped ZTCs	4.4	~1.0	9
Activated templated N-doped carbon	4.5	1.4	10
Polyaniline derived activated carbon	4.3	1.38	11
N-doped activated carbon monoliths	5.14	1.25	12
Activated hierarchical N-doped carbon	4.8	1.4	13
Activated N-doped carbon from algae	4.5	~1.1	14
Compactivated carbons from sawdust	5.8	2.0	15
Fern-derived activated carbon	5.67	~1.7	16
Compactivated carbons from polypyrrole	5.5	2.1	17
Clove-derived activated carbon	5.4	1.4	18
Potassium oxalate-activated carbon from date seed	5.0	1.8	19

References

1. M. Sevilla and A. B. Fuertes, *Energy Environ. Sci.*, 2011, **4**, 1765.
2. J. Silvestre-Albero, A. Wahby, A. Sepulveda-Escribano, M. Martinez-Escandell, K. Kaneko and F. Rodriguez-Reinoso, *Chem. Commun*., 2011, **47**, 6840.
3. N. P. Wickramaratne and M. Jaroniec, *ACS Appl. Mater. Interfaces*, 2013, **5**, 1849.
4. N. P. Wickramaratne and M. Jaroniec, *J. Mater. Chem. A*, 2013, **1**,112.
5. J. Wang, et al, *J. Mater. Chem.*, 2012, **22**, 13911.
6. X. Fan, L. Zhang, G. Zhang, Z. Shu, J. Shi, *Carbon*, 2013, **61**, 423.
7. M. Sevilla, P. Valle-Vigon and A. B. Fuertes, *Adv. Funct. Mater.*, 2011, **21**, 2781.
8. W. Xing, et al, *Energy Environ. Sci.*, 2012, **5**, 7323.
9. Y. D. Xia, R. Mokaya, G. S. Walker and Y. Q. Zhu, *Adv. Energy Mater.*, 2011, **1**, 678.
10. Y. Zhao, L. Zhao, K. X. Yao, Y. Yang, Q. Zhang and Y. Han, *J. Mater. Chem.*, 2012, **22**, 19726.
11. Z. Zhang, et al, *Phys.Chem. Chem. Phys.*, 2013, **15**, 2523
12. M. Nandi, et al, *Chem. Commun.*, 2012, **48**, 10283.
13. D. Lee, C. Zhang, C. Wei, B. L. Ashfeld and H. Gao, *J. Mater. Chem. A*, 2013, **1**, 14862.
14. M. Sevilla, C. Falco, M. M. Titirici and A. B. Fuertes, *RSC Advances*, 2012, **2**, 12792.
15. N. Balahmar, A. C. Mitchell, and R. Mokaya, *Adv. Energy Mater.*, 2015, **5**, 1500867.
16. J. Serafin, K. Kiełbasa and, B. Michalkiewicz, *Chem. Eng. J.*, 2022, **429**, 131751.
17. B. Adeniran and R. Mokaya, *Nano Energy*, 2015, **16**, 173.
18. I. Alali and R. Mokaya, *Energy Environ. Sci.*, 2022, 1**5**, 4710.
19. A. Altwala and R. Mokaya, *RSC Adv*., 2022,**12,** 20080.

Table S2. Packing density and low-pressure volumetric CO_2 uptake, expressed as g l^{-1} (or cm^3 (STP) cm^{-3}), for PPI-derived carbons compared to benchmark carbons and metal organic frameworks (MOFs). The values in parenthesis are volumetric uptake expressed as cm^3 (STP) cm^{-3}.

Sample	Density[a]	Volumetric CO_2 uptake (g l^{-1}) or (cm^3 STP cm^{-3})				Reference
	(g cm^{-3})	0.15 bar	1 bar	5 bar	9 bar	
PPI-600-2	1.10	70 (39)	180 (101)	326 (183)	379 (213)	This work
PPI-700-2	1.04	62 (35)	196 (110)	401 (225)	477 (267)	This work
PPI-800-2	0.92	44 (25)	155 (87)	374 (210)	465 (260)	This work
PPI-900-2	0.87	48 (27)	146 (82)	357 (200)	450 (252)	This work
PPI-1000-2	0.83	40 (22)	133 (74)	334 (187)	429 (240)	This work
ACC2700	0.79	38 (19)	170 (87)	400 (204)	482 (245)	1
ACC2800	0.72	29 (15)	133 (68)	349 (178)	450 (229)	1
HCC2700	0.83	51 (26)	197 (100)	409 (208)	476 (242)	1
HCC2800	0.63	25 (13)	116 (59)	312 (159)	405 (206)	1
SD2600	0.94	54 (27)	178 (91)	315 (160)	348 (177)	2
SD2600P	0.95	80 (41)	242 (123)	370 (188)	399 (203)	2
SD2650	0.89	47 (24)	161 (82)	294 (150)	338 (172)	2
SD2650P	0.81	54 (27)	189 (96)	371 (189)	427 (217)	2
Carbon A1	1.00	38 (19)	157 (80)	278 (142)	316 (161)	3
Carbon A3-36	0.87	27 (14)	128 (65)	302 (154)	378 (192)	3
MOF210	0.25[b]	4 (2)	10 (5)	38 (19)	65 (33)	4
Mg-MOF-74	0.41[c]	103 (52)	144 (73)			5,6

[a] Packing density or tapping density. [b] Crystal density of MOF210. [c] 'Tapping density' of Mg-MOF-74 from reference 5.

References

1. I. Alali and R. Mokaya, *Energy Environ. Sci.*, 2022, **15**, 4710.
2. N. Balahmar, A. C. Mitchell, and R. Mokaya, *Adv. Energy Mater.*, 2015, **5**, 1500867.
3. J. P. Marco-Lozar, M. Kunowsky, F. Suarez-Garcia, J. D. Carruthers and A. Linares-Solano, *Energy Environ. Sci*., 2012, **5**, 9833.
4. H. Furukawa, N. Ko, Y. B. Go, N. Aratani, S. B. Choi, E. Choi, A. O. Yazaydin, R. Q. Snurr, M. O'Keeffe, J. Kim and O. M. Yaghi, *Science*, 2010, **329**, 424.
5. S. R. Caskey, A. G. Wong-Foy and A. J. Matzger, *J. Am. Chem. Soc*., 2008, **130**, 10870.
6. Y. Peng, V. Krungleviciute, I. Eryazici, J. T. Hupp, O. K. Farha and T. Yildirim, *J. Am. Chem. Soc*. 2013, **135**, 11887.

Table S3. Volumetric working capacity, expressed as g l^{-1} (or cm^3 (STP) cm^{-3}) for pressure swing adsorption (PSA) and vacuum swing adsorption (VSA) of CO_2 on PPI-derived carbons compared to benchmark porous materials at ca. 25 ^oC for a pure CO_2 gas stream and a 20% partial CO_2 pressure flue gas stream. The values in parentheses are the working capacity in cm^3 (STP) cm^{-3}

Sample	Density	Pure CO_2[a] (g/l or cm^3 cm^{-3})		Flue gas CO_2[b] (g l^{-1} or cm^3 cm^{-3})		Reference
	(g cm^{-3})	PSA	VSA	PSA	VSA	
PPI-600-2	1.10	163 (91)	180 (101)	114 (64)	106 (59)	This work
PPI-700-2	1.04	229 (128)	212 (119)	137 (77)	100 (56)	This work
PPI-800-2	0.92	247 (138)	188 (105)	125 (70)	70 (39)	This work
PPI-900-2	0.87	240 (135)	160 (90)	108 (60)	73 (41)	This work
PPI-1000-2	0.83	232 (130)	146 (82)	100 (56)	63 (35)	This work
ACC2700	0.79	257 (131)	202 (103)	139 (71)	66 (34)	1
ACC2800	0.72	248 (126)	162 (82)	111 (57)	51 (26)	1
HCC2700	0.83	238 (121)	223 (114)	153 (78)	84 (43)	1
HCC2800	0.63	225 (115)	144 (73)	100 (51)	47 (24)	1
SD2600	0.94	153 (78)	190 (97)	124 (63)	87 (44)	2
SD2600P	0.95	142 (72)	251 (128)	171 (87)	121 (62)	2
SD2650	0.89	149 (76)	180 (92)	121 (62)	74 (38)	2
SD2650P	0.81	143 (73)	213 (108)	143 (73)	86 (44)	2
HKUST-1	0.43	147 (75)	121 (62)	85 (43)	30 (15)	3
Mg-MOF-74	0.41	63 (32)	70 (36)	38 (19)	74 (38)	3
NaX	0.63	44 (22)	78 (40)	50 (26)	69 (35)	4

[a]1 bar to 6 bar for PSA; 0.05 bar to 1.5 bar for VSA. [b]0.2 bar to 1.2 bar for PSA; 0.01 bar to 0.3 bar for VSA.

References

1. I. Alali and R. Mokaya, *Energy Environ. Sci.*, 2022, **15**, 4710.
2. N. Balahmar, A. C. Mitchell, and R. Mokaya, *Adv. Energy Mater.*, 2015, **5**, 1500867.
3. J. M. Simmons, H. Wu, W. Zhou and T. Yildirim, *Energy Environ. Sci*., 2011, **4**, 2177.
4. Y. Belmabkhout, G. Pirngruber, E. Jolimaitre and A. Methivier, *Adsorption*, 2007, **13**, 341.

Table S4. Methane uptake for PPI-derived carbons compared to selected benchmark MOFs and carbons reported in the literature. Volumetric uptake of powder MOFs is calculated based on crystallographic density rather than packing density.

Sample	Density ($g\ cm^{-3}$)	65 bar ($g\ g^{-1}$)	65 bar ($cm^3\ cm^{-3}$)	80 bar ($g\ g^{-1}$)	80 bar ($cm^3\ cm^{-3}$)	100 bar ($g\ g^{-1}$)	100 bar ($cm^3\ cm^{-3}$)	Reference
PPI-800-2	0.92	0.21	270	0.22	287	0.25	309	This work
PPI-900-2	0.87	0.23	283	0.25	303	0.28	331	This work
PPI-1000-2	0.83	0.25	288	0.27	311	0.29	338	This work
CHCC2800	0.82	0.26	293	0.28	315	0.30	339	1
CHCC4700	0.75	0.27	282	0.29	306	0.32	334	1
CHCC4800	0.58	0.32	258	0.35	279	0.38	309	1
CNL4800	0.67	0.26	241	0.29	269	0.31	291	2
PPYCNL124	0.52	0.30	217	0.33	238	0.36	260	2
PPYCNL214	0.36	0.36	183	0.41	204	0.46	229	2
ACDS4800	0.69	0.25	243	0.27	262	0.29	282	2,3
PPYSD114	0.47	0.32	211	0.35	231	0.39	254	3
AX-21 carbon	0.487	0.30	203	0.33	222	0.35	238	4
HKUST-1	0.881	0.21	263	0.22	272	0.23	281	4
Ni-MOF-74	1.195	0.15	259	0.16	267	0.17	277	4
Al-soc-MOF-1	0.34	0.41	197	0.47	222			5
MOF-210	0.25	0.41	143	0.48	168			6
NU-1500-Al	0.498	0.29	200	0.31	216	0.34	237	7
NU-1501-Fe	0.299	0.40	168	0.46	193	0.52	218	7
NU-1501-Al	0.283	0.41	163	0.48	190	0.54	214	7
$_{mono}$HKUST-1	1.06	0.17	261	0.18	278	0.18	275	8
$_{mono}$UiO-66_D	1.05	0.14	210	0.17	245	0.20	296	9

References

1. I. Alali and R. Mokaya, *Energy Environ. Sci.*, 2022, **15**, 4710.
2. A. Altwala and R. Mokaya, *J. Mater. Chem. A*, 2022, **10,** 13744.
3. A. Altwala and R. Mokaya, *Energy Environ. Sci.*, 2020, **13**, 2967.
4. J. A. Mason, M. Veenstra and J. R. Long, *Chem. Sci.*, 2014, **5**, 32.
5. D. Alezi, *et al*, *J. Am. Chem. Soc.*, 2015, **137**, 13308.
6. H. Furukawa, *et al*, *Science* 2010, **329**, 424–428.
7. Z. Chen, *et al*, *Science*, 2020, **368**, 297.
8. T. Tian, Z. Zeng, D. Vulpe, M. E. Casco, G. Divitini, P. A. Midgley, J. Silvestre-Albero, J. C. Tan, P. Z. Moghadam and D. Fairen-Jimenez, *Nat. Mater.*, 2018, **17**, 174.
9. B. M. Connolly, M. Aragones-Anglada, J. Gandara-Loe, N. A. Danaf, D. C. Lamb, J. P. Mehta, D. Vulpe, S. Wuttke, J. Silvestre-Albero, P. Z. Moghadam, A. E. H. Wheatley and D. Fairen-Jimenez, *Nat. Commun.*, 2019, **10**, 2345.

Table S5: Methane uptake working capacity for PPI-derived carbons compared to selected benchmark MOFs and carbons reported in the literature.

Sample	65 bar		80 bar		100 bar		Reference
	($g\ g^{-1}$)	($cm^3\ cm^{-3}$)	($g\ g^{-1}$)	($cm^3\ cm^{-3}$)	($g\ g^{-1}$)	($cm^3\ cm^{-3}$)	
PPI-800-2	0.13	174	0.14	190	0.16	212	This work
PPI-900-2	0.15	183	0.17	203	0.19	231	This work
PPI-1000-2	0.17	199	0.19	222	0.21	249	This work
CHCC2800	0.18	200	0.20	222	0.22	246	1
CHCC4700	0.20	210	0.22	234	0.25	262	1
CHCC4800	0.25	197	0.28	218	0.31	248	1
CNL4800	0.19	182	0.22	202	0.24	224	2
PPYCNL124	0.23	167	0.26	188	0.29	209	2
PPYCNL214	0.29	146	0.34	167	0.39	192	2
ACDS4800	0.18	171	0.20	189	0.22	209	2,3
PPYSD114	0.25	162	0.28	182	0.32	205	2
AX-21 carbon	0.23	155	0.26	174	0.28	190	4
HKUST-1	0.15	179	0.16	198	0.17	207	4
Ni-MOF-74	0.08	148	0.09	152	0.10	162	4
Al-soc-MOF-1	0.36	176	0.42	201			5
MOF-210	0.38	134	0.45	157			6
NU-1500-Al	0.24	165	0.26	181	0.29	202	7
NU-1501-Fe	0.36	151	0.42	176	0.48	201	7
NU-1501-Al	0.37	147	0.44	174	0.50	198	7
$_{mono}$HKUST-1	0.12	184	0.13	201	0.13	198	8
$_{mono}$UiO-66_D	0.11	167	0.14	202	0.17	253	9

References

1. I. Alali and R. Mokaya, *Energy Environ. Sci.*, 2022, **15**, 4710.
2. A. Altwala and R. Mokaya, *J. Mater. Chem. A*, 2022, **10,** 13744.
3. A. Altwala and R. Mokaya, *Energy Environ. Sci.*, 2020, **13**, 2967.
4. J. A. Mason, M. Veenstra and J. R. Long, *Chem. Sci.*, 2014, **5**, 32.
5. D. Alezi, *et al*, *J. Am. Chem. Soc.*, 2015, **137**, 13308.
6. H. Furukawa, *et al*, *Science* 2010, **329**, 424–428.
7. Z. Chen, *et al*, *Science*, 2020, **368**, 297.
8. T. Tian, Z. Zeng, D. Vulpe, M. E. Casco, G. Divitini, P. A. Midgley, J. Silvestre-Albero, J. C. Tan, P. Z. Moghadam and D. Fairen-Jimenez, *Nat. Mater.*, 2018, **17**, 174.
9. B. M. Connolly, M. Aragones-Anglada, J. Gandara-Loe, N. A. Danaf, D. C. Lamb, J. P. Mehta, D. Vulpe, S. Wuttke, J. Silvestre-Albero, P. Z. Moghadam, A. E. H. Wheatley and D. Fairen-Jimenez, *Nat. Commun.*, 2019, **10**, 2345.

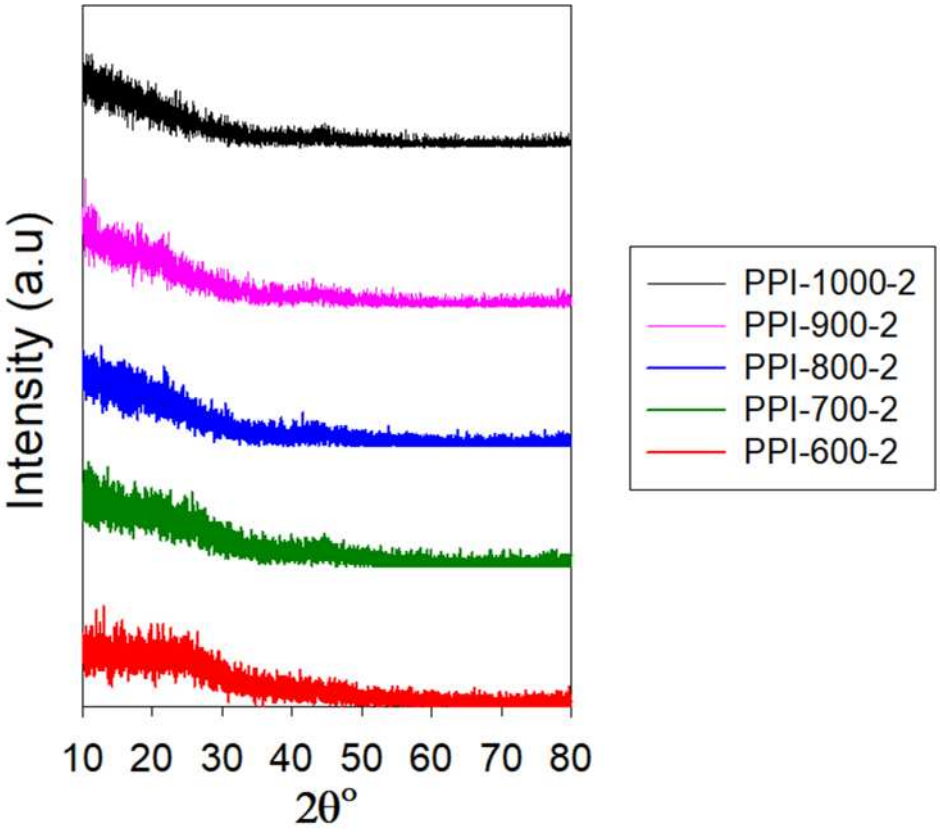

Figure S1. Powder XRD patterns of PPI-derived carbons prepared via carbonisation for 2 h at 600 to 1000 ^{o}C.

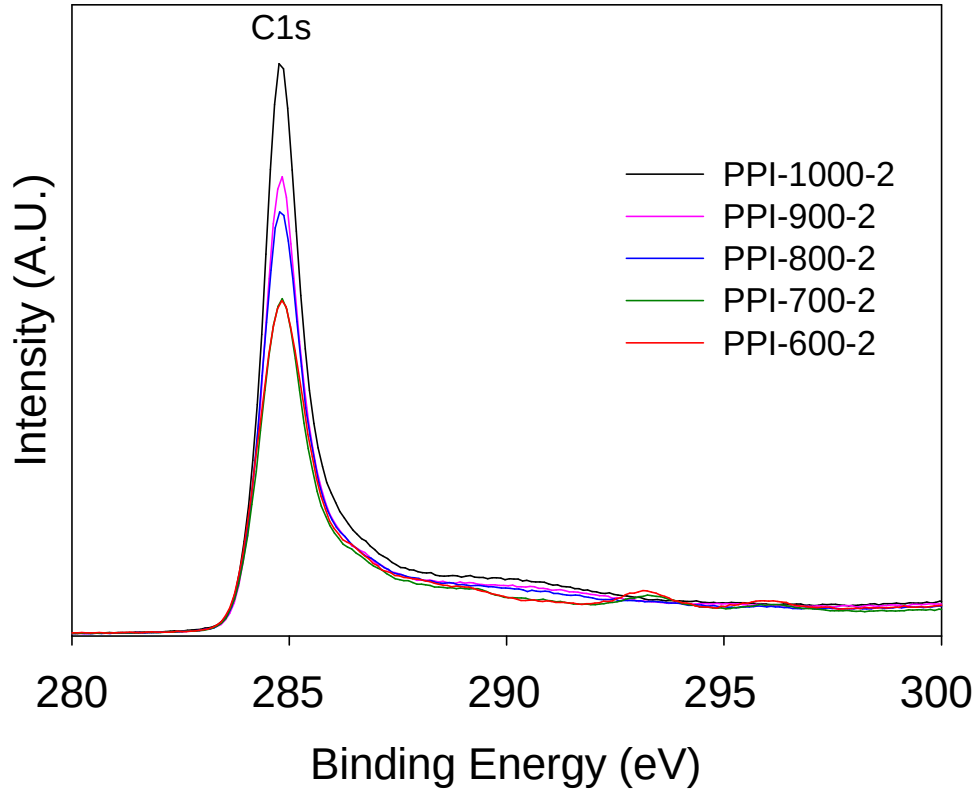

Figure S2. High resolution XPS spectra showing C 1s peak of PPI-derived carbons prepared via carbonisation for 2 h at 600 to 1000 ^{o}C.

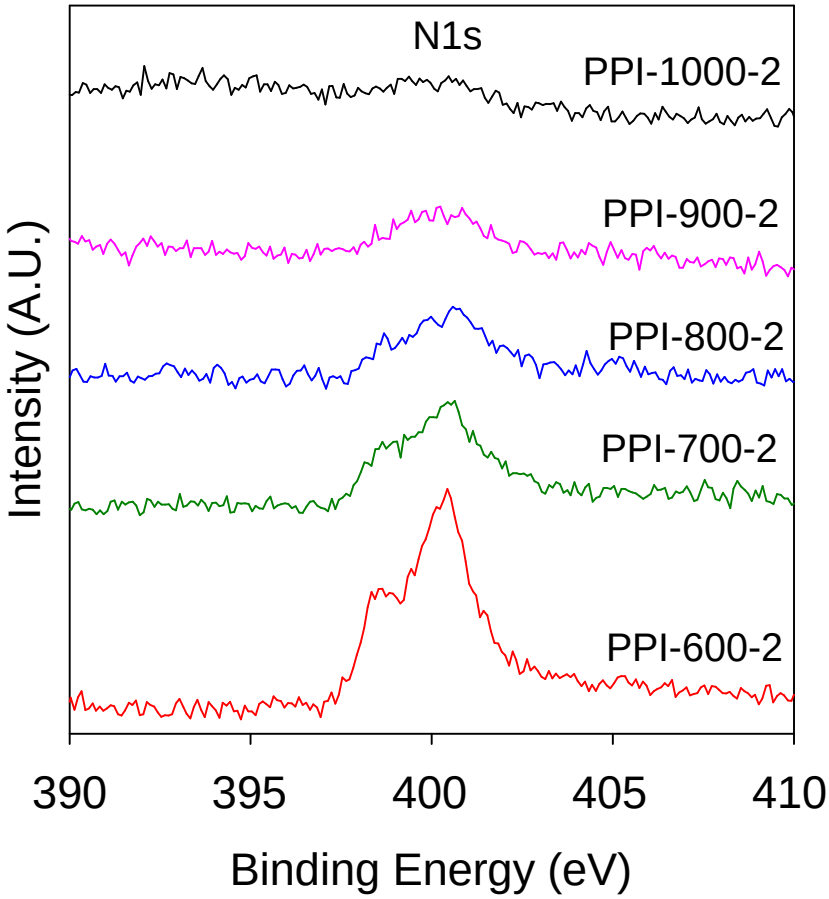

Figure S3. High resolution XPS spectra showing N 1s peak of PPI-derived carbons prepared via carbonisation for 2 h at 600 to 1000 ^{o}C.

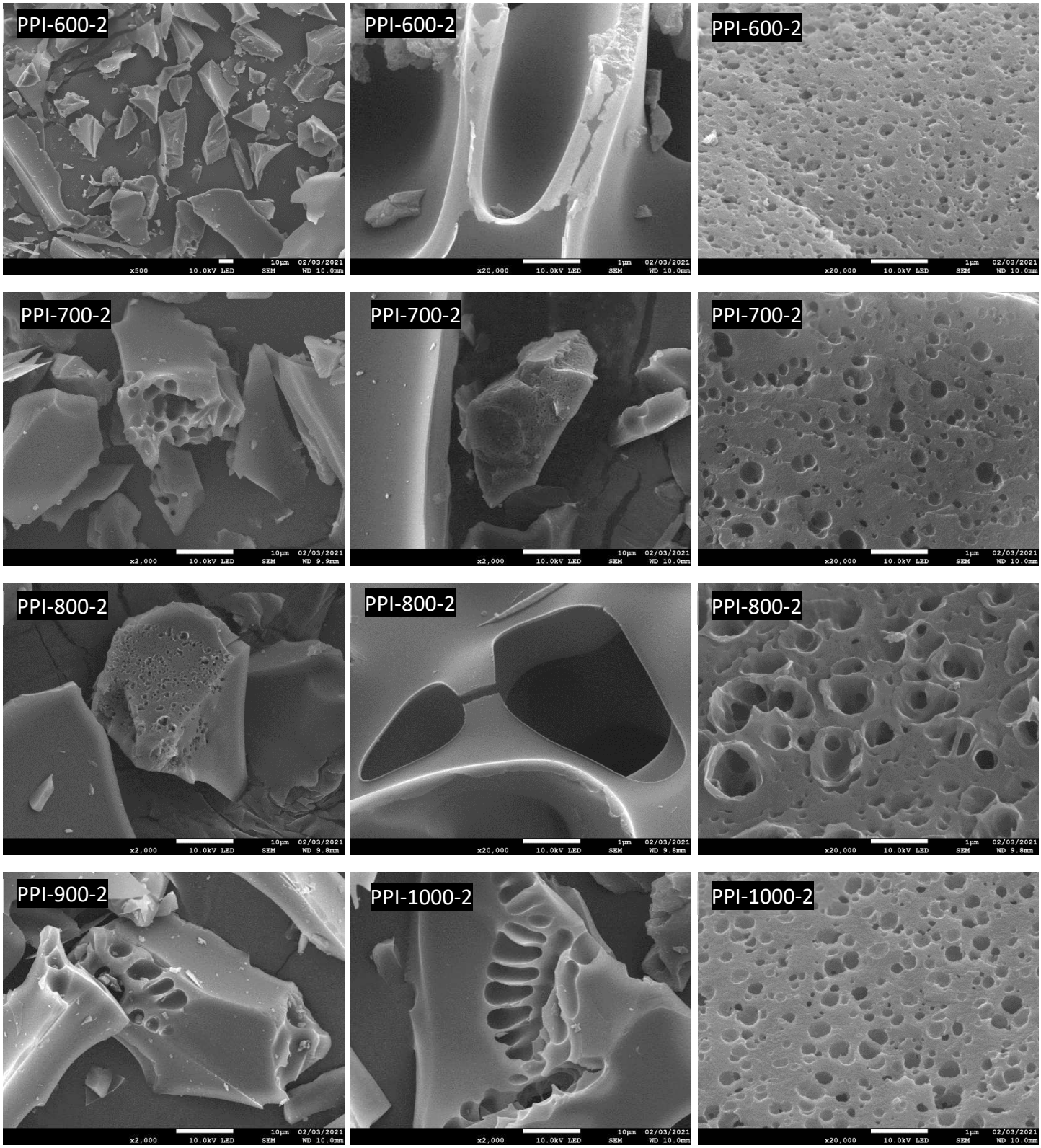

Figure S4. SEM images of PPI-derived carbons

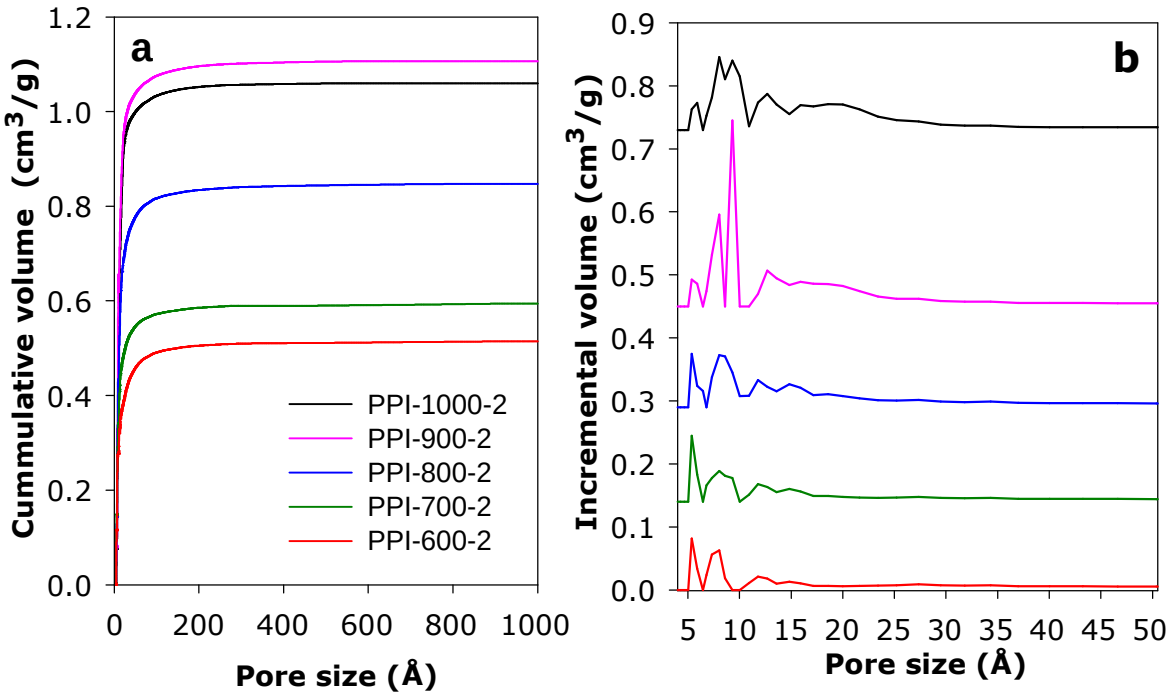

Figure S5. Pore size distribution curves of PPI-derived carbons plotted in (a) cumulative form and (b) differential form. Both plots show that the materials are highly microporous.

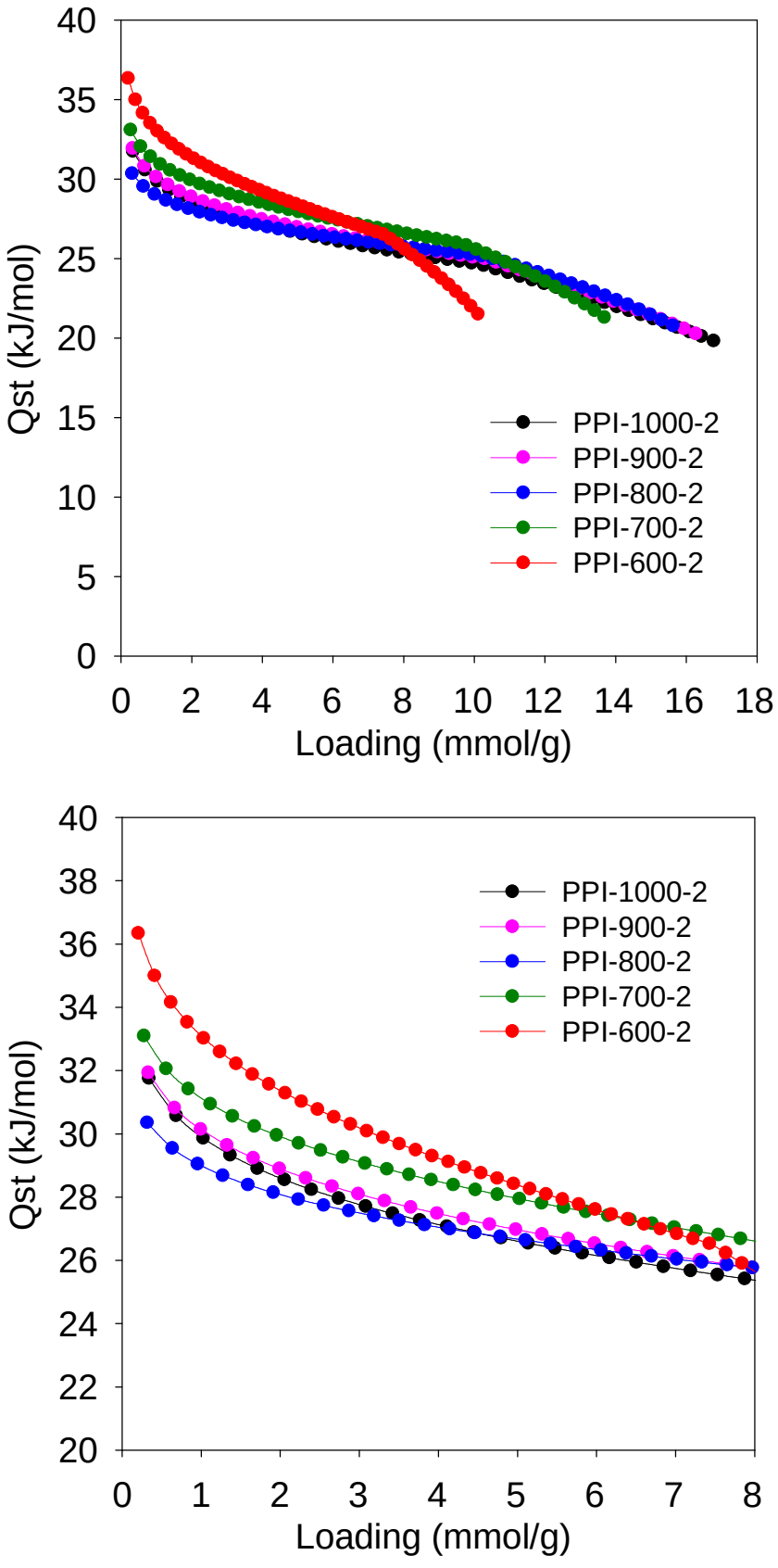

Figure S6. Isosteric heat of adsorption (Qst) of CO_2 on PPI-derived carbons prepared via carbonisation for 2 h at 600 to 1000 ^{o}C. For clarity, the lower panel shows the Qst plots on expanded scales.

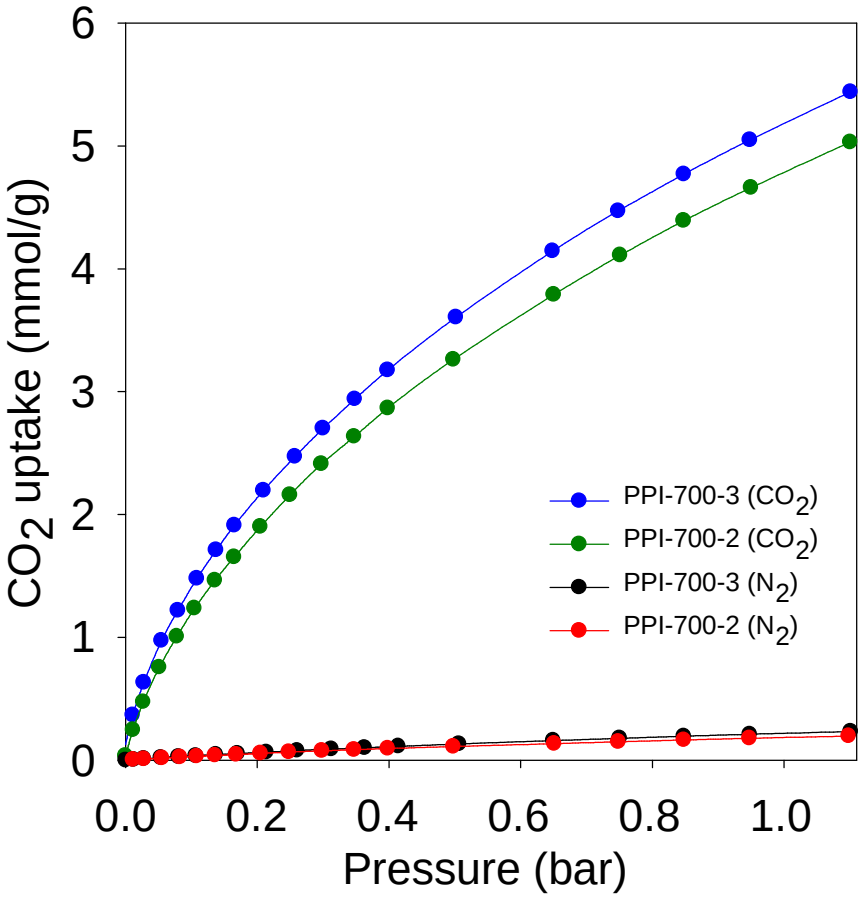

Figure S7. Comparison of CO_2 and N_2 uptake at room temperature for samples PPI-700-2 and PPI-700-3. At 1 bar, the comparison gives a CO_2/N_2 adsorption ratio of 25 for both PPI-700-2 and PPI-700-3.

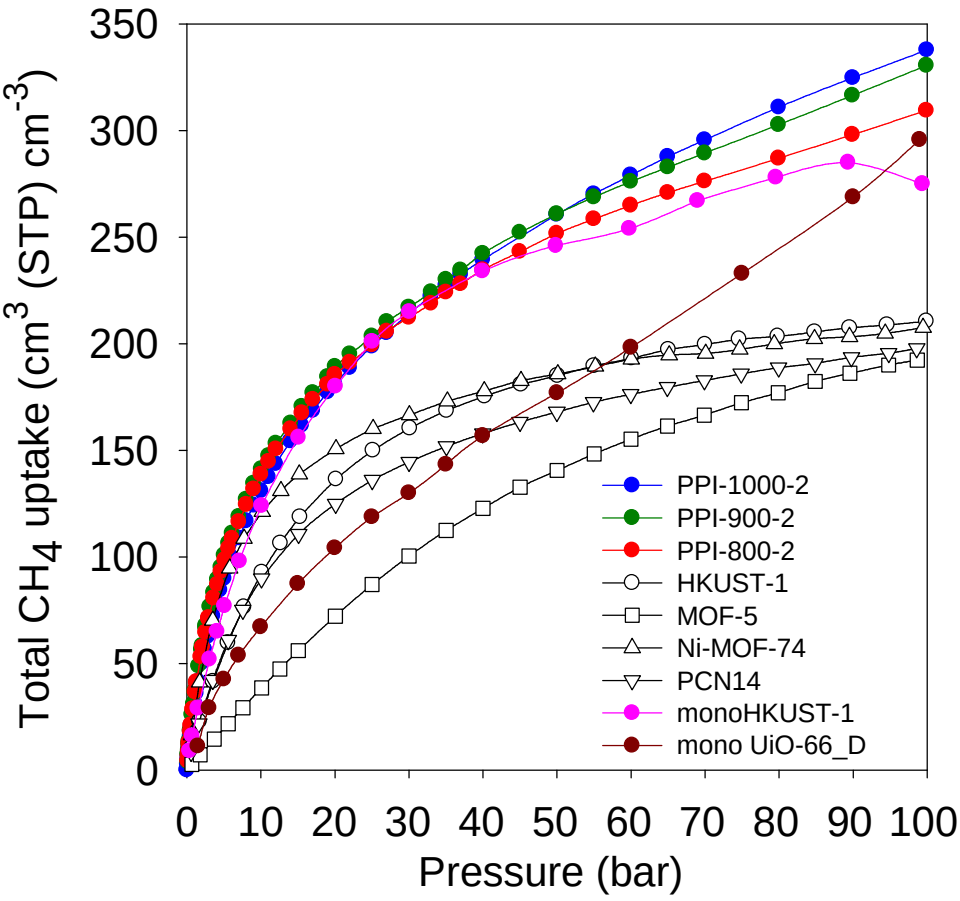

Figure S8. Total volumetric methane uptake of PPI-derived carbons at 25 °C compared to benchmark MOF materials. The uptake of powder MOFs was calculated using crystallographic density and a reduction of 25% was applied to simulate more realistic packing density.